International Journal of Scientific Engineering and Technology (ISSN : 2277-1581)
Volume No.2, Issue No.1, pp : 31-39 1 Jan. 2013

An Optimization Study of Fischer–Tropsch Synthesis Using Commercial Cobalt Catalyst

Hanif A. Choudhury, Vijayanand S. Moholkar
Center for Energy, Indian Institute of Technology Guwahati, Guwahati, Assam, India
vmoholkar@iitg.ac.in

ABSTRACT
Fischer-Tropsch synthesis with a commercial cobalt catalyst (Albemarle) has been carried out under various combinations of two process parameters, viz. reaction pressure and GHSV (gas hourly space velocity) using synthesis gas with molar ratio of $H_2/CO = 2$. The optimum set of reaction parameters that yielded hydrocarbon product in the desired carbon number range of C_{10}-C_{14} and chain growth probability factor of 0.62 was: pressure = 3 MPa, GHSV = 3600 h^{-1} and temp = 493 K. In the pressure range of 1-2 MPa at lower GHSV of 1800 h^{-1}, products obtained were in the carbon number range of C_{14}-C_{24}. An analysis of the link between operating parameters and product distribution has also been given using alkyl mechanism of FT synthesis and Blyholder model for adsorption of CO on metal sites.

Key words: Fischer-Tropsch synthesis, cobalt catalyst, Alkyl mechanism, GHSV

1. Introduction

Fischer–Tropsch synthesis (FTS) is a well known process for production hydrocarbons from synthesis gas derived from different sources such as coal gasification, natural gas reforming, biomass gasification [1]. Recently, the interest of scientific and industrial community in Fischer–Tropsch (F–T) synthesis has been renewed due to fast depletion of fossil fuels, fluctuating prices of crude oil and concerns of global warming due to greenhouse gas emission. Last decade has seen immense research activity worldwide in development of as well as implantation of various renewable energy technologies, such as solar, wind, and biofuels. Despite these efforts only a small fraction of total energy demand is met through renewable sources. As per the report of US Department of Energy (DoE), a cumulative contribution of solar, wind and biofuels is 1.5% of the energy consumption of USA [2]. The major energy needs of our society are in terms of electricity and transportation fuel. The F–T synthesis tries to fulfill the latter need due to its ability of manufacturing synthetic diesel and gasoline through renewable energy sources such as biomass gasification. FT technology also gives opportunity to utilize remote and inaccessible energy sources such as reserves of natural gas by setting local plants for conversion of natural gas to synthesis gas and further liquefaction of this gas to diesel and gasoline. Similarly, gasification facilities can also be set up near remote or deep coal deposits with further liquefaction of this gas to transportation fuels through FT technology [3].

FT synthesis is essentially a catalytic reaction. The active and selective catalysts for the FT reaction are mainly based on cobalt or iron. Cobalt–based catalysts are very popular since they are promising for long–chain hydrocarbon synthesis [4-5]. Supported cobalt catalysts have been extensively studied for Fischer–Tropsch synthesis (FTS) because of their higher activity compared to iron catalysts [5–6]. The FT synthesis process involves simultaneous large number of reactions and the product spectrum consisting of a complex multi component mixture of linear and branched hydrocarbons and oxygenated products. Thus, the selectivity of the products (and not mere the extent yield or conversion) is a crucial facet of an efficient and viable FT technology. Main products of the FT synthesis are linear paraffins and □□olefins. The general reactions of FTS are summarized as follows:

Paraffins:

$$(2n+1)H_2 + nCO \longrightarrow C_nH_{2n+2} + nH_2O \qquad \text{(R.1)}$$

Olefins:

$$2nH_2 + nCO \longrightarrow C_nH_{2n} + nH_2O \qquad \text{(R.2)}$$

Water gas shift reaction:

$$CO + H_2O \rightleftarrows CO_2 + H_2 \qquad \text{(R.3)}$$

Oxygenates:

$$2nH_2 + nCO \longrightarrow C_nH_{2n}O + (n\text{-}1)\,H_2O \qquad \text{(R.4)}$$

Type, composition and nature of catalyst govern the selectivity of products from FT process, and hence, proper selection of catalyst as well as optimization of the process conditions is of vital importance in FT process.

The carbon number of the product hydrocarbon (either chain or branched hydrocarbon) is determined by the process conditions, viz. temperature, pressure and space velocity. Increase in temperature results in shifts towards the product with lower carbon number. Several previous authors have described the effect of these parameters on the yield and selectivity of the FT process. Dictor and Bel [7], Donnelly and Scatterfield [8], Mirzaei et al. [9] and Anderson [10] have studied the effect of temperature on FT

synthesis. They observed an increase of olefin to paraffin ratio with increasing temperature for potassium promoted precipitated iron catalyst. Effect of total pressure on the product selectivity on alkaline promoted iron catalyst has been reported by Dry [11]. Donnelly and Scatterfield [8] found that increasing the H_2/CO ratio in the reactor feed results in production of lighter hydrocarbon (with lower carbon number). The influence of the space velocity (or in other words, residence time) of the synthesis gas on the selectivity has been investigated by Bukur et al. [12]. Kuipers et al. [13] have investigated increase in the olefin to paraffin ratio with increasing space velocity (and hence, resulting in decrease of the conversion due to smaller residence time) on a poly–crystalline cobalt foil. Similar studies have also been done by Bukur et al. [12] on a commercial (Ruhrchemie) supported iron catalyst (Fe/Cu/K/SiO_2), and Iglesia et al. [14] on TiO_2–supported ruthenium catalysts. Bukur et al. [12] have reported no effect of the space velocity on the molecular weight (i.e. the carbon number) of the hydrocarbons, while Iglesia et al. [14] have observed an increase in the average molecular weight of the products with decrease of the space velocity. The selectivity to methane and olefins has been reported to reduce with decreasing space velocity, while the selectivity towards paraffins remains unchanged.

In this study, we have attempted to optimize the FT process using commercial cobalt catalyst procured from Albemarle, Netherlands using a fixed bed reactor. The optimization variables are pressure and space velocity. The temperature of the process has been kept constant, as the effect of temperature on product distribution is well known [15], in that higher temperatures favor smaller carbon number hydrocarbons. The physical cause leading to this effect is higher desorption of tendency of the reactants from catalyst surface at elevated temperature. This optimization study will give insight into the variation in product selectivity in terms of carbon number with optimization parameters using stoichiometric synthesis gas with ratio of H_2 to CO as 2:1. Such a study is also important for the best and effective use of the cobalt catalyst, taking into consideration high cost of cobalt.

2. Experimental

2.1. Catalyst

The cobalt based catalyst was procured from M/s Albemarle, Netherlands. The exact composition of the catalyst was not undisclosed to us under the terms and conditions of an agreement between Albemarle and the Indian Institute of Technology Guwahati. However, BET and TPR study of the catalyst was done in order to understand the surface and reduction property of the catalyst, which is a prerequisite for any heterogeneous catalyst.

2.2 Catalyst characterization

Temperature programmed reduction (TPR) was performed using Micromeritics TPD/TPR 2720 system to determine reducibility of cobalt catalyst. The catalyst (0.3 g) was reduced in a flow of 5% H_2/Ar (30 cm^3/min) with a ramp rate of 10 ^oC/min to 1073 K. A thermal conductivity detector (TCD) was used to measure H_2 consumption. The detector output was calibrated based upon 100% reducibility of Ag_2O powder, and a H_2O trap was used to remove H_2O produced during the reduction. The degree of reduction of the catalyst was calculated by using data of TPR measurements as follows [16]:

$$\% \text{ reduction} = \frac{H_2 \text{ consumption below 723 K}}{\text{Total } H_2 \text{ consumption in TPR experiment}} \times 100 \quad (1)$$

2.3 Experimental set–up and protocol

***Experimental Set–up*:** A schematic diagram of the reactor and its accessories is shown in Figure 1. A fixed bed tubular reactor (MOC: SS 316, thickness: 2 mm, ID: 6.35 mm or ¼ in.) was used for all reactions. The reactor had two gas supply lines of 6.35 mm (¼ in.) ID, each for purge gas (nitrogen) and synthesis gas (mixture of CO and H_2). The synthesis gas supply line was wrapped with thermal tapes so as to preheat the feed gas to 423 K. The reactor effluent line (ID 6.35 mm) was also heated in a similar manner to 373 K to avoid any condensation of the product in the line prior to back–pressure regulator valve. Thereafter, no thermal wrapping was given to the product lines, thus maintaining the temperature in them at ambient condition, where higher hydrocarbon products can condense. The liquid product was collected in a trap (gas–liquid separator) kept at ambient temperature. Cold water (at 298 K) was circulated in a jacket around the trap so as to achieve maximum possible condensation of the hydrocarbon products. The lighter hydrocarbons and unreacted reactant gases are removed from the trap and purged through a gas flow meter. The flow rate of feed synthesis gas was controlled using mass flow controller (Make: Eureka Ml Flow, Range: 0–500 cm^3/min). Catalyst (1 g) was placed inside the reactor enclosed between glass wool plugs. The catalyst was reduced in situ at 673 K for 12 h under a stream of 50% H_2 and N_2 mixture (0.1 MPa pressure, 15 ml/min). After 12 h of reduction, the temperature was reduced to 473 K under the constant flow of hydrogen. Synthesis gas was introduced at a particular space velocity (GHSV), and pressure was gradually increased and set at the desired value. The temperature inside the reactor was monitored using two thermocouples, one at the catalyst bed and other at the surface of reactor. These temperatures were maintained constant by circulating

cooling water through a thermal jacket (in the form of ⅛ in. copper tubing) wrapped around the reactor. Experiments were performed for five different combinations of reaction pressure and GHSV. The conditions for each of the five experiments are listed in Table 1 and designated as protocols 1 to 5.

Materials: All gases used were procured from M/s Vadilal Gas Ltd. (Gujarat, India, purity: 99.999%). The gas cylinders containing reaction mixture (H_2/CO = 67%/33% v/v) were connected to gas supply lines through two–stage high pressure regulator. The analyses of the gaseous products in the reactor effluent were performed by an online gas chromatograph (Make: Thermo Fischer Ceres 800 Plus system) using Porapack–Q column provided with a thermal conductivity detector (TCD). The liquids products were also analyzed by the same GC provided with a flame ionization detector (FID) using BP–10.5 column. For characterization of gas chromatograph, hydrocarbon standards in the carbon number range of C5-C24 were procured from Sigma-Aldrich.

Analysis:

1. The CO conversion (%) has been calculated according to the following equation:

$$\text{CO conversion} = \frac{(n_{CO})_{in} - (n_{CO})_{out}}{(n_{CO})_{in}} \times 100 \quad (2)$$

2. The molar selectivity toward the individual components on carbon basis has been calculated according to the equation:

$$m_i = \frac{y_i}{\sum_{j=1}^{n} y_i} \quad (3)$$

y_i = mole fraction of component *i* in reactor effluent

3. Results and Discussion

3.1 The reduction profile and the surface properties of the catalyst

TPR profile of the cobalt oxide catalyst is depicted in Figure 2. It can be observed that the reduction process of the catalyst occurs in two distinct stages. The first peak near 573 K is ascribed to the transformation of Co_3O_4 to CoO, whereas the second peak near 743 K represents the transformation of CoO to Co [17,18]. The proposed scheme for the reduction of cobalt oxides might be written as follows:

$$Co_3O_4 \xrightarrow{H_2} 3\,CoO + H_2O \quad \text{(first stage at 573 K)} \quad \text{(R.5)}$$

$$3\,CoO \xrightarrow{3H_2} 3\,CO + 2\,H_2O \quad \text{(second stage between 720 and 770 K)} \quad \text{(R.6)}$$

Based on calculations according to equation 1, the reducibility the cobalt catalyst was found to be 33%. For BET (Brunauer–Emmett–Teller) surface area determination of the catalyst, 0.3 g catalyst sample was degassed at 423 K for 2 h, and then heated at 10 K/min to 423 K and held for 2 h before analysis. The BET surface area of the catalyst was determined as 190 m^2/g by N_2 physisorption at 77 K (Make: Beckcoulter). Despite having large surface area, the lower reducibility of the catalyst could be due to difficulty in the reduction of CoO to Co.

3.2 Effect of operation conditions on product profile

To identify and optimize the process condition of Fischer–Tropsch reaction, effects of pressure and the gas flow rate (GHSV) on selectivity of the products were investigated. The results of reactions conducted at different conditions were adjudged and compared with yardsticks of overall CO conversion and selectivity for hydrocarbons in the desired carbon number range.

***Effect of total reaction pressure*:** FTS reaction is essentially a polymerization type reaction, in which the $–CH_2–$ units formed from adsorbed CO and H_2 reactant gases add up to form hydrocarbons of different chain length. Thus, as evident from reactions R.1, the numbers of product moles in FTS reaction are less than reactant moles resulting in positive pressure–dependence, as per Le Chatelier's principle. An obvious consequence of these effects is that increase of reaction pressure also promotes the FTS reaction, leading to an increase in the CO conversion. With increasing pressure, longer chain hydrocarbons are likely to form that could possibly condense and saturate the catalyst pores by liquid product. To assess effect of reaction pressure on product selectivity, we have carried out a series of reactions at reaction pressure range of 1 to 3 MPa using synthesis gas with molar ratio of H_2/CO as 2:1 and temperature of 493 ± 10 K. At each reaction pressure, the reduced catalyst was tested for 10 h. The results are presented in the Fig. 3 for reaction pressures of 1, 1.5 and 2 MPa, respectively, at GHSV of 1800 h^{-1}. It is clearly observed that with the increase in the total pressure, there is an increase in the carbon number of the product, i.e. longer chain hydrocarbons that condense at ambient temperature. This also shows increasing trend in liquefaction of synthesis gas with rising reaction pressure. At a reaction pressure of 1 MPa, the product molar selectivity is toward C_{12}. An increase in the pressure to 1.5 MPa shifts the product molar selectivity towards the longer hydrocarbons (in the range C_{16}–C_{18}), which is evident from the product profiles depicted in Fig. 3. Further increase in the pressure to 2 MPa

shows interesting trend in that highest selectivity is seen for C_{24} with moderate selectivities in the range of C_{14}–C_{16}; while selectivity in the intermediate carbon number range of C_{18}–C_{22} is, however, lower than both C_{14}–C_{16} and C_{24}. At constant GHSV of 1800 h^{-1}, the rise in reaction pressure from 1 to 2 MPa increased CO conversion by approximately 30%.

An explanation for the observed results can be given as follows: As per the alkyl mechanism Figure 4, the FT reaction is essentially a chain polymerization type reaction which is initiated by chemisorption of the carbon monoxide on the catalyst surface. The carbon monoxide is believed to have dissociative adsorption on the catalyst surface. Adsorption of carbon monoxide on the cobalt catalyst surface has been reported to be on the on–top site of Co(0001) [19], which is mainly due to interaction between filled 5□□orbital and the double degenerated 2□ □ orbital [20] and the center of the metal d–band as shown in Figure 5. Charge is donated from carbon to the metal by the 5σ bond and stabilized by back-donation from the metal d-orbitals to the $2\pi^*$ antibonding molecular orbitals, weakening the CO bond. Dissociation of chemisorbed CO results in formation of surface carbon and surface oxygen. The surface oxygen is removed either by adsorbed hydrogen (with formation of water) or adsorbed CO (with formation of CO_2) [21]. The surface carbon, on the other hand, can undergo sequential hydrogenation to yield intermediate methylidyne (CH), methylene (CH_2) and methyl (CH_3) species. In the overall FTS reaction, the CH_3 surface species plays role of initiator, while CH_2 surface species plays role of monomer. These species react (either by β–hydrogen abstraction or hydrogen addition) to form long chain hydrocarbon products, either α–olefin or n–paraffins. A higher pressure causes greater adsorption of carbon monoxide on the catalyst surface, causing greater formation of surface species (CH, CH_2 and CH_3), and greater extent of reaction among them to form hydrocarbon product with higher carbon number (or a longer chain hydrocarbon). Hence with increase in the pressure the product selectivity increases towards the longer hydrocarbons.

Effect of synthesis gas flow rate: Gas flow rate in the reactions has been measured in terms of the gas hour space velocity (GHSV). The GHSV influences the residence time of the gas with the catalyst. To understand the possible effect of GHSV on the selectivity of the products in terms of carbon number, we have done experiments at 7 different GHSVs, viz. 24000, 19200, 14400, 9600, 4800, 3600 and 1800 h^{-1}. In the GHSV range of 24000 h^{-1} to 4800 h^{-1}, no liquid hydrocarbon products were obtained. This essentially means that no FTS reaction occurred for these gas hour space velocities. Even if any FTS reaction occurred, the yields of gaseous products would have been in too low concentrations to be detected by the gas chromatograph. Further reduction of GHSV in the range of 3600–1800 h^{-1}, significant fraction of liquid hydrocarbons (C_{5+}) were observed in the product. The effect of GHSV on the selectivity of products can be deduced from product profile depicted in Fig. 3. It could be inferred that an increase in reaction pressure from 2 to 3 MPa at a constant GHSV of 3600 h^{-1}, the carbon number range of the product increases from C_6–C_{10} to C_{10}–C_{14}. Similarly, at a constant pressure of 2 MPa, reduction in the GHSV from 3600 to 1800 h^{-1} results in significant rise in the carbon number of product from C_6–C_{10} to C_{14}–C_{24}. These results show that the product distribution of the FT reaction in terms of carbon number is dominated by combined effect of reaction pressure and GHSV.

An explanation to these results can be given as follows: With higher residence time, there is longer interaction between catalyst particles and the gas molecules leading to higher adsorption of the reactant molecules. This phenomenon also leads to prolongation of the residence time of reactants and reaction intermediates on the catalyst surface causing further hydrogenation and oligomerization of short–chain hydrocarbons resulting in long chain products (C_{5+}) that condense at ambient conditions. Similar observations have been made in previous studies by Dictor and Bell [7], Donnely and Satterfield [8], Bukur et al. [12], Kuipers et al. [13] and Wang et al. [22] have also reported decrease in the olefin to paraffin ratio of the product with decreasing space velocity, indicating re–adsorption of olefins and further hydrogenation to paraffins.

4. Conclusion

Present study using commercial cobalt catalyst has attempted to optimize two important process parameters of FT synthesis, viz. the total reaction pressure and the residence time. Interesting trends in the product profile of the FTS reaction were observed from a set of experiments with permutation-combination of above-mentioned parameters. Main goal of our experiments was to deduce the influence of GHSV and reaction pressure on product profile, and optimize the reaction conditions for products with carbon number C_{12} or higher, which is the typical range of hydrocarbons in diesel. Among the range of reaction pressures and GHSV attempted in this work, reaction pressure range of 1–2 MPa with GHSV 1800 h^{-1} as in protocol 1, 2 and 3 gives maximum selectivity towards C_{14}–C_{24}. Moving towards a higher reaction pressure of 3 MPa, with a faster GHSV of 3600 h^{-1} or higher as in protocol 5, the products selectivity shifts in the desired range C_{10}–C_{14} although CO conversion is to some extent lesser than

protocols 1, 2 and 3. Thus, the optimum set of parameters for the FT process with commercial catalyst used in this work is found to be pressure of 3 MPa and GHSV of 3600 h^{-1}. We believe that these results will be useful for design and optimization of a large scale FT using the same catalyst.

Acknowledgement

This research was supported by Ministry of New and Renewable Energy, Government of India under grant no. 19/20/2007-R&D/BE dated 06.08.2008.

References

i. Keshav TR, Basu S (2007) Gas-to-liquid technologies: India's perspective. Fuel Processing Technology 88:93-500
ii. Hsin Chen W, Chung Chen J, Tsai CD, Jiang TL (2007) Transient gasification and syngas formation from coal particles in a fixed-bed reactor. International journal of energy research. 31(9):895-911
iii. Tremel A, Gaderer M, Spliethoff H (2012) Small-scale production of synthetic natural gas by allothermal biomass gasification. International Journal of Energy Research. doi:10.1002/er.2933.
iv. Hook M, Aleklett K (2010) A review on coal-to-liquid fuels and its coal consumption. International Journal of Energy Research 34(10):848-864
v. Buragohain B, Mahanta P, Moholkar VS (2012) Performance correlations for biomass gasifiers using semi-equilibrium non-stoichiometric thermodynamic models. International Journal of Energy Research 36(5):590-618
vi. Wei Guo K (2012) Green nanotechnology of trends in future energy: a review. International Journal of Energy Research 36(1):1-17
vii. Ranjan A, Moholkar VS (2011) Biobutanol: science, engineering, and economics. International Journal of Energy Research 36(3):277-323
viii. Dry ME (2002) The Fischer–Tropsch process: 1950–2000. Catalysis Today 71: 227-241
ix. Khodakov AY, Chu W, Fongarland P (2007) Advances in the development of novel cobalt Fischer−Tropsch catalysts for synthesis of long-chain hydrocarbons and clean fuels. Chemical Reviews 107, 1692-1744
x. Tre´panier M, Dalai AK, Abatzoglou N (2010) Synthesis of CNT-supported cobalt nanoparticle catalysts using a microemulsion technique: Role of nanoparticle size on reducibility, activity and selectivity in Fischer–Tropsch reactions. Applied Catalysis A: General 374:79–86
xi. Davis BH (2001) Fischer–Tropsch synthesis: current mechanism and futuristic needs. Fuel Processing Technology 71:157-166
xii. Hammer H, Joisten M, Lüngen S, Winkler D (1994) New zeolites in fischer-tropsch synthesis. International Journal of Energy Research 18(2):223-231
xiii. Baerns M, Guan N, Körting E, Lindner U, Lohrengel M, Papp H (1994) Catalyst development for selective conversion of syngas to mainly aromatic hydrocarbons. International Journal of Energy Research 18(2):197-204
xiv. Dictor RA, Bell AT (1986) Fischer–Tropsch synthesis over reduced and unreduced iron oxide catalysts. Journal of Catalysis 97:121–136
xv. Donnelly TJ and Satterfield CN (1989) Product distributions of the Fischer–Tropsch synthesis on precipitated iron catalysts. Applied Catalysis A: General 52:93–114
xvi. Mirzaei AA, Babaei AB, Galavy M, Youssefi A(2010) A silica supported Fe–Co bimetallic catalyst prepared by the sol/gel technique: Operating conditions, catalytic properties and characterization. Fuel Processing Technology 91:335–347
xvii. Anderson RB (1956) Catalysts for the Fischer–Tropsch Synthesis (Vol. 4). New York,Van Nostrand Reinhold
xviii. Dry ME (1981) The Fischer–Tropsch Synthesis. In: Anderson JR, Boudart M (eds.)Catalysis Science and Technology, vol. 1, 160–255. New York: Springer–Verlag
xix. Bukur DB, Patel S A, Lang X (1990) Fixed bed and slurry reactor studies of Fischer–Tropsch synthesis on precipitated iron catalyst. Applied Catalysis A: General 61:329–349
xx. Kuipers EW, Scheper C, Wilson JH, Oosterbeek H (1996) Non–ASF product distributions due to secondary reactions during Fischer–Tropsch synthesis. Journal of Catalysis 158:288–300
xxi. Iglesia E, Reyes SC, Madon RJ (1991) Transport–enhanced α–olefin readsorption pathways Ru–catalyzed hydrocarbon synthesis. Journal of Catalysis 129:238–256
xxii. Yan Z, Wang Z, Bukur DB, Goodman DW (2009) Fischer–Tropsch synthesis on a model Co/SiO2 catalyst. Journal of Catalysis 268:196–200
xxiii. Kang SH (2010) ZSM-5 supported iron catalysts for Fischer–Tropsch production of light olefin. Fuel Processing Technology 91: 399–403

xxiv. Saib A M, Claeys M, van Stenn E (2002) Silica supported cobalt Fischer–Tropsch catalysts: Effect of pore diameter of support. Catalysis Today 71:395–402

xxv. Song D, Li J (2006) Effect of catalyst pore size on the catalytic performance of silica supported cobalt Fischer–Tropsch catalysts. Journal of Molecular Catalysis A: Chemical 247: 206–212

xxvi. Lahtinen J, Vaari J, Kauraala K, Soares EA, van Hove MA (2000) LEED investigations on Co(0001): the (3×3)R30°-CO overlayer. Surface Science 448: 269–278

xxvii. van Daelen, M A, Li YS, Newsam JM, van Santen RA (1994) Transition states for NO and CO dissociation on Cu(100) and Cu(111) surfaces. Chemical Physics Letters 226: 100-105

xxviii. Ribeiro MC, Jacobs G, Davis BH, Cronauer DC, Kropf AJ, Marshall CL (2010) Fischer–Tropsch synthesis: An in-situ TPR-EXAFS / XANES investigation of the influence of group I alkali promoters on the local atomic and electronic structure of carburized iron/silica catalysts. Journal of Physical Chemistry C 114:7895-7903

xxix. Pour A N, Shahri SMK, Zamani Yand Zamanian A (2010) Promoter effect on the CO_2-H_2O formation during Fischer-Tropsch synthesis on iron-based catalysts. Journal of Natural Gas Chemistry 19:193-197

xxx. Wang ZX, Dong T, Yuan LX, Kan T, Zhu XF, Torimoto Y, Sadakata M, Li QX (2007) Characteristics of bio-oil-syngas and its utilization in Fischer-Tropsch synthesis. Energy & Fuels 21: 2421-2432

xxxi. Pour AN, Housaindokht MR, Tayyari SF, Zarkesh J (2010) Effect of nano-particle size on product distribution and kinetic parameters of Fe/Cu/La catalyst in Fischer-Tropsch synthesis. Journal of Natural Gas Chemistry 19:107–116

Table 1: FTS reaction data at different Pressure and GHSV

Protocol	Pressure (MPa)	CO Conversion %	GHSV(h^{-1})	Molar Selectivity
Protocol 1	1	28	1800	$C_{12} - C_{16}$
Protocol 2	1.5	34	1800	$C_{16} - C_{20}$
Protocol 3	2	37	1800	$C_{14} - C_{24}$
Protocol 4	2	27	3600	$C_6 - C_{10}$
Protocol 5	3	27	3600	$C_{10} - C_{14}$

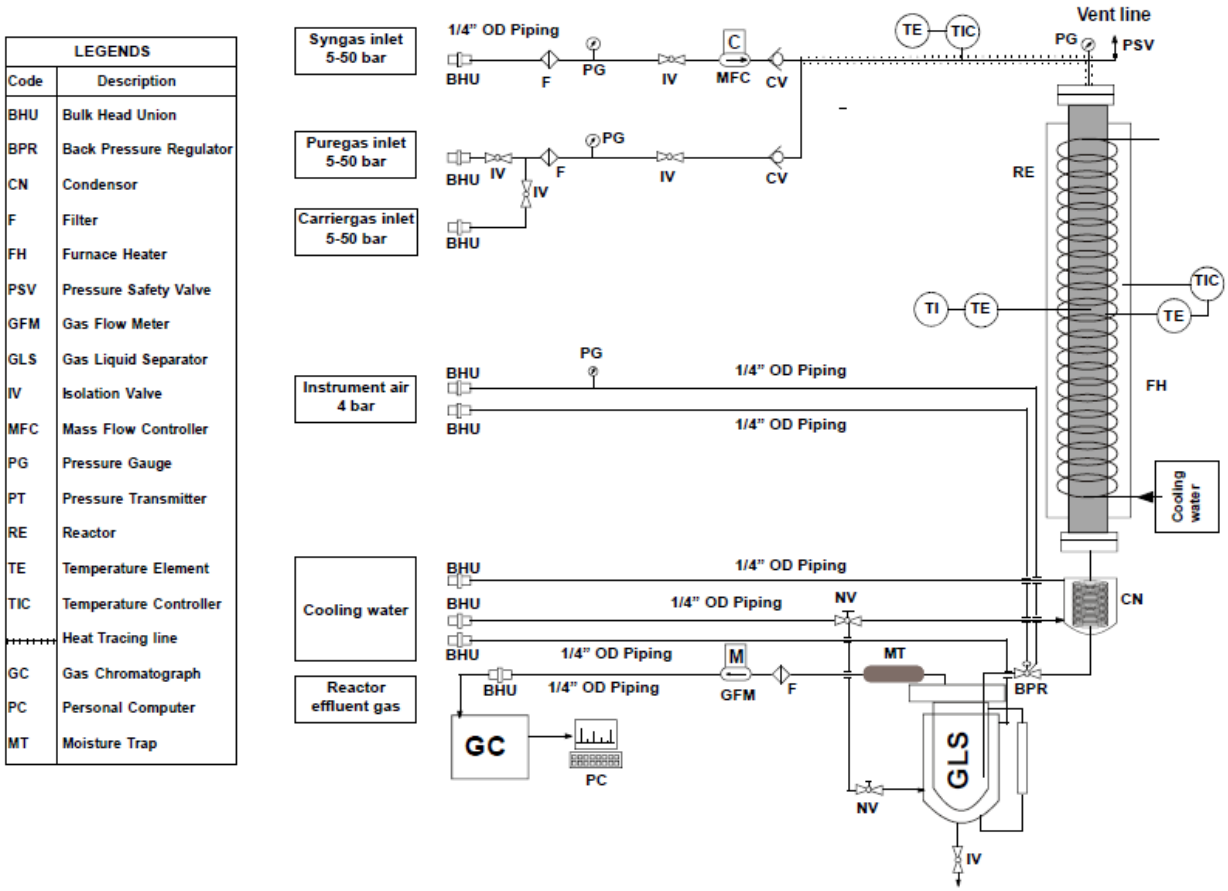

Figure 1: Experimental setup

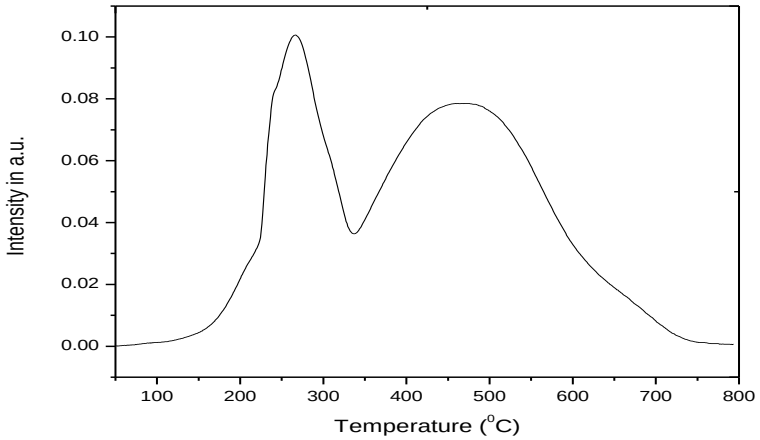

Figure 2: TPR profile of Cobalt catalyst

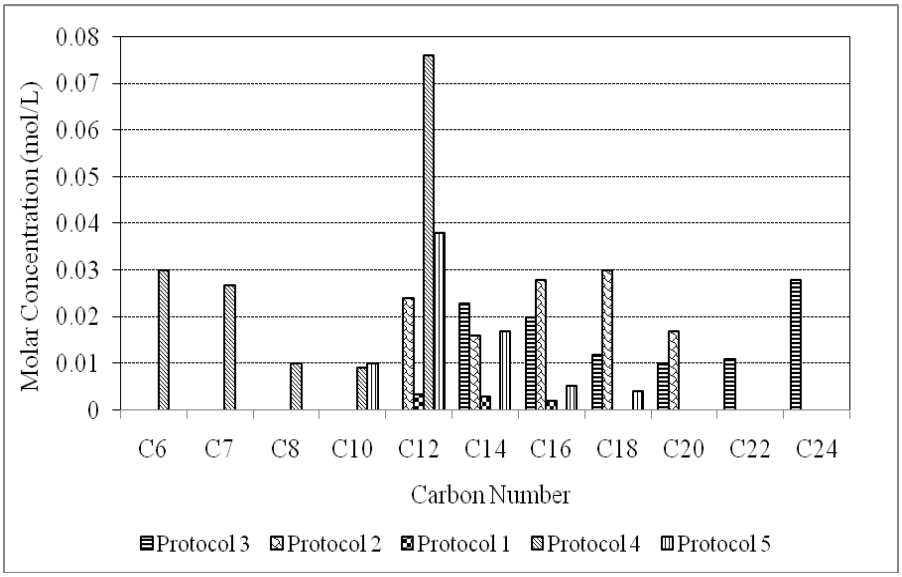

Figure 3. Product profile and distribution in different experimental protocols

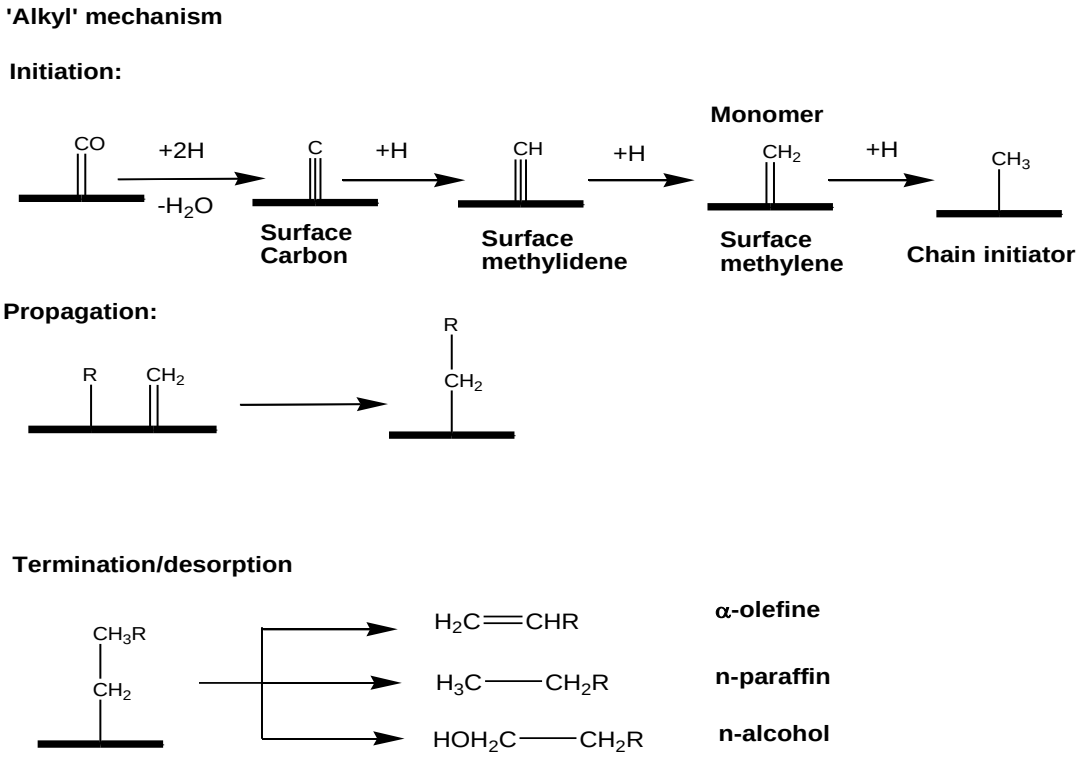

Figure 4. Alkyl mechanism

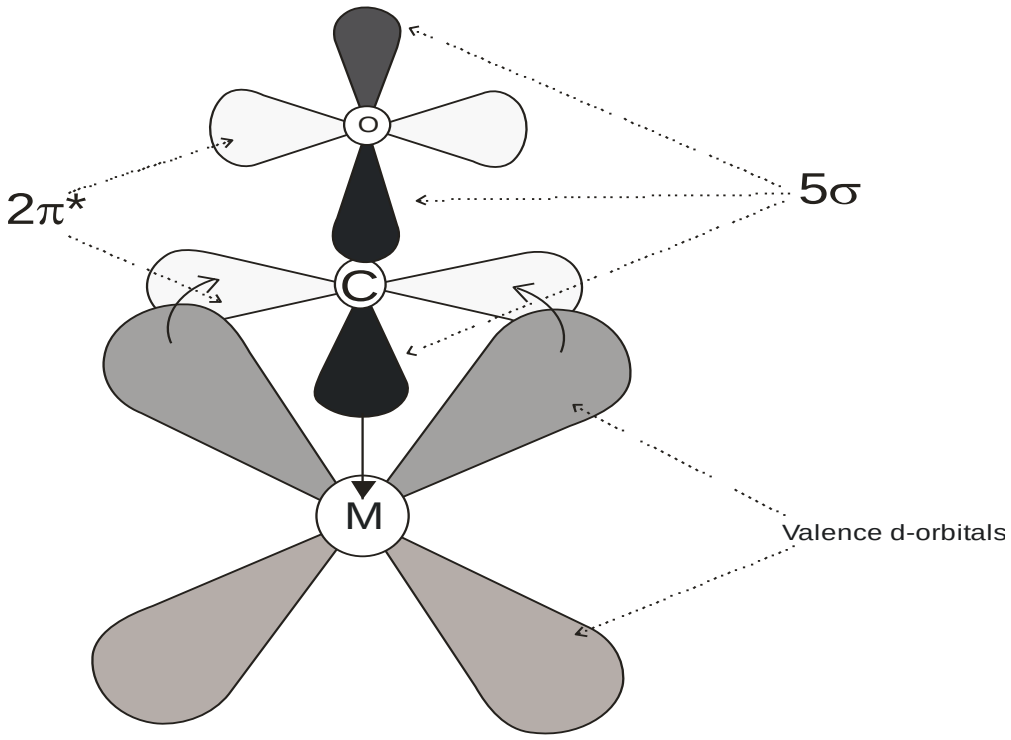

Figure 5. Molecular orbital diagram of CO to a metal site according to the Blyholder model. (redrawn with modifcations from ref. [24]).